Full length article

A decade of China's air quality monitoring data suggests health impacts are no longer declining

Ben Silver *, Carly L. Reddington, Yue Chen, Steve R. Arnold

School of Earth and Environment, University of Leeds, Woodhouse Lane, Leeds LS2 9JT, UK

A B S T R A C T

China's national air quality monitoring network has revealed a rapid improvement in air quality during the 2010s, during which fine particulate matter ($PM_{2.5}$) and other priority pollutant levels fell, except for ozone, which concurrently increased. However, recent changes in China's economic outlook mean that the future trajectory of China's air quality is highly uncertain. Here we analyse the last 10 years of air quality monitoring data to assess whether China's air quality has continued to improve in recent years. We find that the period of steep negative trends in $PM_{2.5}$ observed during 2014–2019 ($-2.47\ \mu g\ m^{-3}\ year^{-1}$) has ended, slowing to $-0.18\ \mu g\ m^{-3}\ year^{-1}$ during 2021–2024. Meanwhile, ozone levels continued to increase during 2021–2024, with a trend of $2.06\ \mu g\ m^{-3}\ year^{-1}$. We demonstrate that population $PM_{2.5}$ exposure in China can be accurately constrained using only surface monitoring station data, and we use this to estimate future health impacts under three observationally-based future $PM_{2.5}$ scenarios. We show that the current government $PM_{2.5}$ reduction target is insufficient to sustain the decrease in $PM_{2.5}$-attributed mortality that was achieved during 2014–2019, and a ∼2 times more ambitious target is needed to offset the effects of China's ageing population.

1. Background

Although it has rapidly improved in recent years, poor air quality remains a serious environmental concern in China, with long-term exposure to fine particulate pollution ($PM_{2.5}$) being the fourth highest risk factor for deaths and years lived with disability, while ozone exposure ranks as the twentieth (Zhou et al., 2019). China no longer suffers from the most $PM_{2.5}$-attributed deaths globally, having been overtaken by India (Li et al., 2023), but China is still estimated to suffer the largest burden in terms of the economic costs to healthcare (Yin et al., 2021). China has recently announced a new target of achieving national average $PM_{2.5}$ concentrations of $25\ \mu g\ m^{-3}$ by 2035 (Reuters, 2024), and aims to peak its CO_2 emissions by 2030 (Green and Stern, 2017). However, as the country faces economic challenges, balancing environmental commitments with maintaining economic growth may become more challenging (Chai et al., 2021).

China's air quality rapidly deteriorated alongside its rapid economic growth during the 1980s and 1990s (Li et al., 2016; Qu and Han, 2021). The 2000s ushered in a period of greater government attention to air pollution controls, initially focussed on reducing acid rain (Hao et al., 2001). This period saw greater enforcement of air quality standards, an increase in monitoring, and a start to the rollout of air pollution control technologies (Beyer, 2006; Florig et al., 2002; Schreifels et al., 2012). The 11th Five Year Plan (2006–2010) is seen as a turning point where air quality control policy began to be prioritised, with air quality

improvement targets becoming mandatory for local governments (Lu et al., 2020; Schreifels et al., 2012). By the end of the decade, it was clear that measures such as the implementation of flue gas desulphurisation on coal-fired power plants had resulted in reduced SO_2 concentrations (Krotkov et al., 2016; Lu et al., 2010; Schreifels et al., 2012; Silver, 2021; Wang et al., 2014). In contrast, observations during this period showed that $PM_{2.5}$, ozone and NO_2 concentrations were continuing to increase across much of China (Chang et al., 2017; Han et al., 2015; Krotkov et al., 2016; Ma et al., 2016; Peng et al., 2016; Verstraeten et al., 2015), as rapid development continued, and air quality control policies had not yet begun to seriously address sources of these pollutants (Jin et al., 2016).

$PM_{2.5}$ concentrations continued to increase until around 2013 (Ma et al., 2019). Public concern over poor air quality began to put pressure on the government to implement policies to control poor air quality (Brimblecombe and Zong, 2019; Jin et al., 2011; Lu et al., 2018; Zhang et al., 2018). Following an episode of severe haze that affected 800 million people across much of Northern and Eastern China (Ferreri et al., 2018; Huang et al., 2015), the government issued the 'Air Pollution Prevention and Control Action Plan' (henceforth, the 'Action Plan'), containing measures to rapidly reduce $PM_{2.5}$ concentrations by controlling emissions from the industrial, transport, and domestic sectors (Jin et al., 2016; Zheng et al., 2018). Control of China's air quality monitoring stations was centralised under the China National Centre for Environmental Monitoring (CNEMC) and the monitoring network was

---

expanded, with >1300 monitoring stations included from 2015 (Luo et al., 2022). The centralisation of the monitoring network helped to avoid local government data manipulation that had resulted in somewhat unreliable data (Andrews, 2008; Ghanem and Zhang, 2014; Stoerk, 2016), although there is evidence to suggest that some manipulation may have continued (Ravetti et al., 2019; Turiel and Kaufmann, 2021).

Air pollutant measurement data from the CNEMC network has shown that after the Action Plan was implemented, $PM_{2.5}$ concentrations began to fall rapidly (Kong et al., 2021; Shi et al., 2021; Silver et al., 2018), with trends of -6% yr^{-1} observed during 2015–2019 (Silver et al., 2020). The steep decrease has been confirmed by satellite observation studies (He et al., 2021; Ma et al., 2019), and is supported by bottom-up emission estimates (Zheng et al., 2018). Using satellite data, He et al. (2021) estimated that $PM_{2.5}$ concentrations fell by $\sim 5\%$ $year^{-1}$ from 45 to 36 μg m^{-3} during 2013–2017. Zheng et al. (2018) estimated changes in anthropogenic emissions in China during 2010–2017, finding that there were substantial decreases of $PM_{2.5}$ (27%), PM_{10} (38%), SO_2 (62%) and NO_x (17%) emissions.

The majority of the mortality burden due to chronic air pollution exposure is attributed to $PM_{2.5}$ (Wang et al., 2020). As a result of the rapid decrease of $PM_{2.5}$, the estimated number of annual $PM_{2.5}$-attributed deaths in China has fallen during the 2010s (Yin, 2022), by 188 thousand during 2012–2019 (Conibear et al., 2022b). Despite the 36% decrease in $PM_{2.5}$ exposure during this period, attributed deaths only decreased by 9%, partly due to China's ageing and increasing population, but also due to the sublinear relationship between $PM_{2.5}$ exposure and health risk (Burnett et al., 2018; Conibear et al., 2022b). However, since $PM_{2.5}$ health impact estimation typically relies on emission inventory or reanalysis datasets which can take several years to prepare, recent reliable estimates of the health impact are currently unavailable.

Meanwhile, tropospheric ozone, another pollutant known to be harmful to human health (Zhang et al., 2019), has seen long-term and widespread increases in China. Ozone also damages vegetation, which adds to food security pressures in China (Li et al., 2024; Tai et al., 2021). Ozone-attributed mortalities in China are estimated to be around an order of magnitude lower than those attributed to $PM_{2.5}$ (Conibear et al., 2022b; Wang et al., 2020) Background (non-urban) monitoring sites have recorded positive trends in ozone since the 1990s (Wang et al., 2009; Xu et al., 2016), which were confirmed by satellite observations that became available during the 2000s (Verstraeten et al., 2015). Ozone concentrations have continued to increase since the 2013 Action Plan, with the CNEMC network recording a trend of 2.2 ppbv $year^{-1}$ in maximum daily 8-hour mean (MDA8) ozone during 2013–2019 (Lu et al., 2020; Silver, 2021).

A key driver of the increase in ozone is the effects of emission controls on abundances of its precursors, having successfully reduced NO_x emissions, while not alleviating emissions of volatile organic compounds (VOC; Zheng et al., 2018). Additionally, modelling studies have suggested that the reduction in $PM_{2.5}$ concentrations has resulted in an increase in ozone formation rates, due to the resulting decrease in heterogeneous loss of hydroperoxyl radicals (Ivatt et al., 2022; Li et al., 2019; Liu and Wang, 2020) and modified absorption and scattering of sunlight (Xing et al., 2017). Modelling studies predict that ozone levels are now peaking, as precursor emission-driven decreases in ozone begin to outweigh the increases due to aerosol-attributed effects (Liu et al., 2023; Wang et al., 2023). However, the future trajectory of ozone remains highly uncertain due to the uncertainties remaining in model representations of ozone chemistry and interactions with aerosols (Dyson et al., 2023; Tan et al., 2020).

In recent years, global and domestic headwinds have buffeted China's economy, potentially changing the trajectory of its air pollutant emissions. The COVID-19 pandemic and its associated lockdowns resulted in short-term impacts on air quality. From early 2020, lockdowns substantially decreased activity, reducing pollutant emissions from residential, industrial, transport and power generation sectors (Zheng et al., 2021). This resulted in short-term decreases in pollutant concentrations, particularly NO_2 (He et al., 2020; Silver et al., 2020). Emissions had mostly returned to normal by the end of 2020 (Zheng et al., 2021), and economic stimulus helped growth rebound during 2021 (Jiang et al., 2022; IMF, 2023). Nevertheless the GDP growth rate has continued on its long-term decreasing trend, falling from 10.6% $year^{-1}$ in 2010 to 5.0% $year^{-1}$ in 2023 (IMF, 2023). The near-future outlook for China's pollutant emissions is unclear under the opposing pressures of continuing emissions mitigation while arresting the decline in economic growth.

Despite surface observations being essential to understanding the processes governing air pollution in China, which has a significant impact on global atmospheric chemistry and climate (Lin et al., 2012; Liu and Matsui, 2021; Zhang et al., 2021), the CNEMC network's data remains difficult for the research community to access. The official government platform, https://air.cnemc.cn:18007/, does not provide access to historical data, with only the most recent 24h of data being available to view. Furthermore, it does not provide an 'Application Programming Interface' to facilitate data access. These barriers to data access and sharing mean that the scientific community lacks an up-to-date understanding of the latest trends in air quality in China. Recent evidence indicates that long-term trends may have been interrupted or reversed in recent years (Li and Zheng, 2023; Wang et al., 2023).

Here, we perform the first trend analysis of 10 years of China's air quality data, using a non-linear method to reveal potential changes or reversals in trends. We comprehensively analyse the CNEMC data to show up-to-date non-linear trends to December 2024, following a comprehensive check and cleaning of the data for the presence of anomalies. We also release this data to the public, in an easy-to-use format, incorporating the inclusion of data quality flags. Furthermore, we demonstrate that China population $PM_{2.5}$ exposure and associated health impact can be accurately quantified using the CNEMC network concentrations in place of gridded data, and we exploit this to inform future $PM_{2.5}$ exposure scenarios. Using these scenarios, along with existing demographic projections, we estimate the future health impact in three scenarios covering a range of plausible exposure trajectories up to 2035.

2. Methods

2.1. Obtaining CNEMC data

Most studies cite the official website, https://air.cnemc.cn:18007/, as being the source of their CNEMC data, with a literature search for journal articles containing "cnemc.cn" returning 482 results (scopus.com, accessed 16/09/2024). However, though the website does display real-time data, as of August 2024, historical data are not available to be downloaded from this website, making the actual source of data unclear. The next most commonly cited source of CNEMC data is third party websites. These websites 'scrape' global air quality data from official websites in real time, accumulating a data record which is made publicly available to download via 'Application Programming Interfaces' (APIs). Examples of these websites include https://aqicn.org/ (AQICN) and https://openaq.org/ (OpenAQ). A literature search finds 268 journal articles containing the keywords 'China air quality' cite one of these two websites as their data source (scopus.com, accessed 16/09/2024). However, currently AQICN does not provide access to historical air pollutant data in original units at hourly time resolution, and OpenAQ no longer collects China's data. Some third-party organisations profit by offering the data for a fee (e.g. https://data.epmap.org/product/nationair).

We obtain CNEMC data from https://quotsoft.net/ (last accessed 2025–01-03; formerly known as https://beijingair.sinaapp.com/), which scrapes data from CNEMC and makes it available to download from Baidu drives, which are difficult to access for those outside China. Although unofficial, this website has been a commonly used source for researchers within China, with a literature search for 'beijingair.

sinaapp' or 'quotsoft.net' returning 88 results (scopus.com, accessed 16/09/2024) with 82 of these including at least one author from a Chinese institution.

We downloaded all historical air quality data from May 13th 2014 to 4th January 2025, obtaining > 0.81 billion hourly measurements of $PM_{2.5}$, PM_{10}, NO_2, ozone, SO_2 and CO concentrations. Since NO data is not available, we are limited to discussing trends in NO_2 rather than NO_x. The data are supplied with a metadata file containing the latitude and longitude coordinates of >2000 air quality monitoring stations.

2.2. Correcting for measurement protocol change

As highlighted by Jin et al. (2020), China updated its air pollutant measurement protocols in September 2018, and began using measured temperature and pressure to calculate aerosol pollutant ($PM_{2.5}$ and PM_{10}) concentrations, rather than reference conditions of 0 °C and 1013.25 hPa, which had previously been used. Furthermore, for gaseous pollutants (ozone, NO_2, SO_2 and CO), the reference temperature was updated to 25 °C. We use formulae based on the ideal gas law provided by Jin et al. (2020) to harmonise pre-protocol change measurements with those taken after the change. To correct measurements of aerosol pollutants, we downloaded hourly ERA5 (Hersbach et al., 2020) surface temperature and pressure and estimated their values at the location of each monitoring station using bilinear interpolation. Typically, the correction reduces pollutant concentrations, with adjusted concentrations prior to the change being on average 7–9% lower depending on species, and up to 43% lower for aerosol pollutants at some stations.

2.3. Data cleaning procedure

As the CNEMC data released in real-time is not subject to quality control, it is necessary to thoroughly check the data for outliers and data quality issues which can influence the estimated trends if not accounted for. To ensure the data used to estimate trends is of good quality, we remove any measurement time series that have high proportions of missing or anomalous data. The data cleaning process is described below and fully summarised in Table 1.

First, we remove stations with high proportions of missing data and station time series that are too short to extract a meaningful non-linear trend. Most of the stations have some missing data, with a median 93.5% of hourly data available between the first and last reported measurement. Some of the records have large gaps (i.e., a period without any reported measurements), which can result in large increases in estimated trend uncertainty when included in the trend-analysis dataset. Around 10% of measurement station time series have a gap longer than a month, and ~1% longer than a year. Using a set of thresholds, we remove time series if: 1) There is <90% of data available between the first and last valid measurement, 2) the time series is <7 years long between its first and last valid measurement or 3) the data has a period without any data for >60 days.

Second, we identify and remove anomalous data. Previous studies have identified several types of outliers in the data that are caused by equipment malfunctions (Rohde and Muller, 2015; Silver et al., 2018; Wu et al., 2018). To detect these outliers, we implement a modified version of the method developed by Wu et al. (2018), which they term 'Probabilistic Automatic Outlier Detection' (PAOD). Briefly, PAOD relies upon normalising air pollutant measurements by calculating their residual in terms of a z-score within a rolling window. In the PAOD method, the expected positive lognormal distribution of air pollutant measurements is used to calculate the probability that a given observation is one of five types of outlier: 1) an extreme value, 2) is significantly different to spatial and temporally neighbouring values, 3) in periods of very low variance, 4) an outlier caused by equipment calibration, and 5) when the PM_{10} concentration $<$ $PM_{2.5}$ concentration. We make several modifications to the PAOD technique in order to reduce the frequency of 'false positives.' We also do not flag PM_{10}

Table 1

Data cleaning. The table shows average values of data availability statistics, as well as the number of stations removed at each stage of the data cleaning process. Where no unit is given, the cell shows the number of stations that pass a particular quality control test.

	$PM_{2.5}$	PM_{10}	NO_2	SO_2	CO	Ozone
initial stations	2031	2031	2031	2031	2031	2031
median length (years)	10	10	10	10	10	10
median data availability (%)	95.0	92.2	95.3	95.5	95.2	95.0
First Availability Check						
>90% data available	1843	1397	1862	1874	1861	1843
>7 years length	1361	1361	1361	1361	1361	1361
no gap > 60 days	1893	1894	1897	1895	1894	1896
remaining stations	1239	916	1257	1258	1251	1249
PAOD (median outliers per station)						
Extreme	2.4	4.4	0.5	7.5	2.3	0.1
Spatio-temporal	3.0	4.2	0.8	6.6	2.8	0.6
Low variance	0.6	1.1	1.3	1.7	0.4	2.8
Diurnal	0.0	0.0	0.0	0.0	0.2	0.0
Second Availability Check						
>0.5% PAOD detected	1228	904	1240	1217	1237	1218
>85% data available	1239	916	1257	1258	1251	1249
>7 years length	1238	910	1257	1257	1249	1249
no gap > 60 days	1239	916	1257	1258	1251	1249
remaining stations	1227	898	1240	1216	1235	1218
remaining data availability (%)	95.0	92.8	95.3	95.3	95.1	95.0

concentrations as outliers when they are lower than $PM_{2.5}$ concentrations. These outliers occur at a high frequency, indicating that PM_{10} concentrations measured by the CNEMC network are often inaccurate, as the equipment used to measure PM_{10} is older (Wu et al., 2018). However, this issue likely affects PM_{10} measurements throughout the time series, not only when PM_{10} $<$ $PM_{2.5}$, therefore it will not improve the PM_{10} trend accuracy to remove these outliers. Our modified version of the PAOD method is fully described in the Supplementary Methods 1 and the number of outliers detected for each pollutant is shown in Supplementary Fig. 1.

Finally, we repeat the first step using the same criteria, to remove station time series that now have lower than needed data availability due to outlier removal. Additionally, we remove time series that have had >0.5% of their data flagged as outliers, as this often indicates the entire time series is unreliable.

2.4. Seasonality and trend extraction using LOWESS

Locally Weighted Scatterplot Smoothing, known as LOWESS, is an algorithm for fitting a smooth curve to data by performing a series of weighted regressions on subsets of the data (Cleveland, 1979). An advantage of LOWESS is that it is a non-parametric method, so does not require that the data be normally distributed. Unlike polynomial-curve fitting, it requires no prior assumptions of the shape of the resulting trend, so it can accommodate multiple reversals in trend direction if necessary. LOWESS has previously been used as part of a common algorithm for time series decomposition (Cleveland et al., 1990).

The LOWESS algorithm operates by fitting a weighted polynomial to a rolling subset or "window" of the data points. We use the tri-cube weighting function, and fit first-degree polynomials for each subset of the data. The size of the subset of data points can be adjusted to modify the degree of smoothing. In our analysis, we choose a window size of 4 years, so that seasonal and inter-annual variability is smoothed out, while longer-term, multiannual changes are captured.

Our technique allows for the seasonal component to smoothly evolve over time, and for confidence intervals on the seasonal and trend component to both be calculated. An example of the trend-fitting

procedure is illustrated in Fig. 1. We first take daily means of the time series data. Then, we extract the seasonal cycle by performing a separate LOWESS fit for each day of the year, and its immediate surrounding days, using a centred rolling window. The rolling window has a width of 15 days, with its central (8th) day being the day of the year for which the seasonal component is estimated. A 15-day window width is chosen to so that seasonal variability is captured smoothly on a multi-day time-scale. We perform 100 bootstrap simulations to capture the uncertainty of the fit. For each day of the year, we take the value of the LOWESS fit on that day, and by taking these values for each of the 365 fits, we extract the seasonal cycle. We estimate its confidence limits by taking the 2.5th and 97.5th percentiles from the bootstrap simulations.

To estimate the trend, we interpolate between the fitted values in each day-of-year fit using a Piecewise Cubic Hermite Interpolating Polynomial (PCHIP). This includes extrapolating each day-of-year trend at both ends, by up to 364 days, so that each of the 365 fits overlap. We also perform this for each of the bootstrap simulations to estimate uncertainty in the extrapolation. The 365 fits are then averaged together, to get the overall trend of the time series. The confidence limits are again estimated by taking the 2.5th and 97.5th percentiles of the bootstrap simulations and their interpolated and extrapolated values.

As an example, to calculate the seasonal trend on January 15th, we compute the LOWESS fit using daily means of the 8th to 22nd using data from each year (2015–2024). Assuming all data is available, this gives 150 (15 × 10; window width multiplied by number of years) points on which to perform the fit. These 210 points are then randomly sampled with replacement 100 times, and the 95% confidence intervals are calculated by estimating the 2.5th and 97.5th percentiles of the bootstrap samples on January 15th. Then, the same process is repeated for January 16th, with data from the 9th to the 23rd being included in the window, and so on.

2.5. Linear trend analysis

To be able to quantify the trend over short periods, and plot the geographic distribution of trends, we also calculate linear trends. We use a similar method to our previous work (Silver et al., 2020), however in this analysis we use the trend and seasonal fit calculated in the previous step to deseasonalise the data. We use the Theil-Sen estimator (Sen, 1968) from the Python package *statsmodels* (Seabold and Perktold, 2010), and assess trend significance using a modified version of the Mann-Kendall test (Hussain and Mahmud, 2019) that accounts for autocorrelation (Hamed and Rao, 1998). For this analysis, we fit the trend to deseasonalised values. The data is deseasonalised using the seasonal and trend fits estimated in non-linear trend extraction step. We take the weekly mean of the deseasonalised data, discarding values where there are fewer than 5 daily mean values present in the week. We calculate the trend if >90% of weeks are valid during the trend period. The confidence limits for the seasonal cycle are used to calculate upper and lower bounds of the Theil-Sen slope.

We quantify linear trends for three 'periods of interest'. The first is '2014–2024,' which includes the entire period of data availability at the time of writing, from May 2014 to December 2024. The second is '2014–2019,' which covers May 2014 to the December 2019. This period is intended to cover the period of rapidly changing concentrations that occurred prior to the start of the COVID-19 pandemic in 2020. The third is 2021–2024, including values from January 2021 to the last available data in December 2024. This period is intended to capture the post-COVID trajectory of air quality trends, which is why we do not include 2020, during which there were widespread lockdowns.

2.6. Averaging of trends

In this work, we present spatially averaged trends across all monitoring stations (that pass quality control tests) in China or its subregions. The CNEMC network in China is distributed throughout the major cities of China, with each city having a number of stations proportional to its population size. Since we include all stations with >7 years of data in the average, the number of stations averaged varies throughout the 10-year period, as some stations join the CNEMC network later in the time series, while others go offline. For this reason, discontinuities are present in the average trend, especially at the start of 2015, as the number of monitoring stations increased by ~60% in this period (Supplementary Fig. 2). As shown in a previous study (Luo et al., 2022), we find that the addition of monitoring stations has a limited effect on average pollutant concentrations.

2.7. Regional groupings of provinces

We divide China into five large regions made from groupings of provinces, to facilitate regional comparison (Supplementary Fig. 3). The most populous and economically active part of China, East China, is divided into two regions, 'Northern East China', and 'Southern East China', which are approximately split at the Qinling-Huaihe Line. 'Northern East China' includes the North China Plain, which contains the Beijing-Tianjin-Hebei region. 'Southern East China' includes the Yangtze River Delta. 'Southwest China' includes the populous Sichuan Basin region. The 'Northeast China' region includes the relatively more densely populated provinces in the northeast of China, while the remaining provinces are grouped into 'Western China,' which includes the relatively sparsely populated provinces to the west of the Hu-Huanyong Line, as well as Inner Mongolia.

2.8. PM$_{2.5}$ health impact estimation

We estimate the health impact of ambient PM$_{2.5}$ using the Global Exposure Mortality Model (Burnett et al., 2018) (GEMM), which has been used to estimate health impacts in China in numerous previous studies (Conibear et al., 2022b; Geng et al., 2021; Li et al., 2023; Shi et al., 2021; Yin et al., 2021; Yin, 2022). Here we estimate the increase in adult (>25 years old) premature deaths from non-communicable diseases and lower respiratory infections (NCD + LRI). Details of the GEMM are fully described in Burnett et al. (2018), the details, assumptions, and limitations relevant to this study are described below.

The GEMM is used to predict the increase in NCD + LRI mortalities relative to the baseline mortality rate. This increase is termed the 'hazard ratio.' The hazard ratio is a function of PM$_{2.5}$ exposure, which increases with PM$_{2.5}$ concentrations greater than the counterfactual concentration of 2.4 µg m^{-3}. The GEMM includes different hazard ratio models for 12 age groups (between 25 and 80+ years) as well as uncertainty intervals (95% confidence limits). Therefore, when combined with time-varying demographic data, the GEMM model can account for the effect of projected ageing on population vulnerability.

As the GEMM estimates the relationship between PM$_{2.5}$ exposure, measured in units of mass concentration, and mortality, it cannot account for the differences in PM toxicity that may occur between regions. We use the version of the GEMM's hazard ratio functions that include data from a Chinese cohort study (Yin et al., 2017). Yin et al (2017) is one of the few cohort studies that has estimated the association between PM$_{2.5}$ exposure and mortality for the very high exposures found in China, and therefore may make the GEMM's estimates more applicable to China's PM$_{2.5}$ composition.

To calculate the excess deaths using GEMM during the period 2000–2035, annual estimates of the population size and mortality rates for the 12 age groups are required, in addition to PM$_{2.5}$ estimates. For age group populations, we use the 'reference' scenario from the Institute for Health Metrics and Evaluation (IHME) (IHME, 2020), which forecasts annual population in each of the twelve age groups until 2100. For the NCD and LRI mortality rates, we use annual Global Burden of Disease (GBD) data (Global Burden of Disease Collaborative Network, 2024) over the period 2000–2021, and projections from the International Futures (IF) model v8.06 (Frederick S. Pardee Center for International
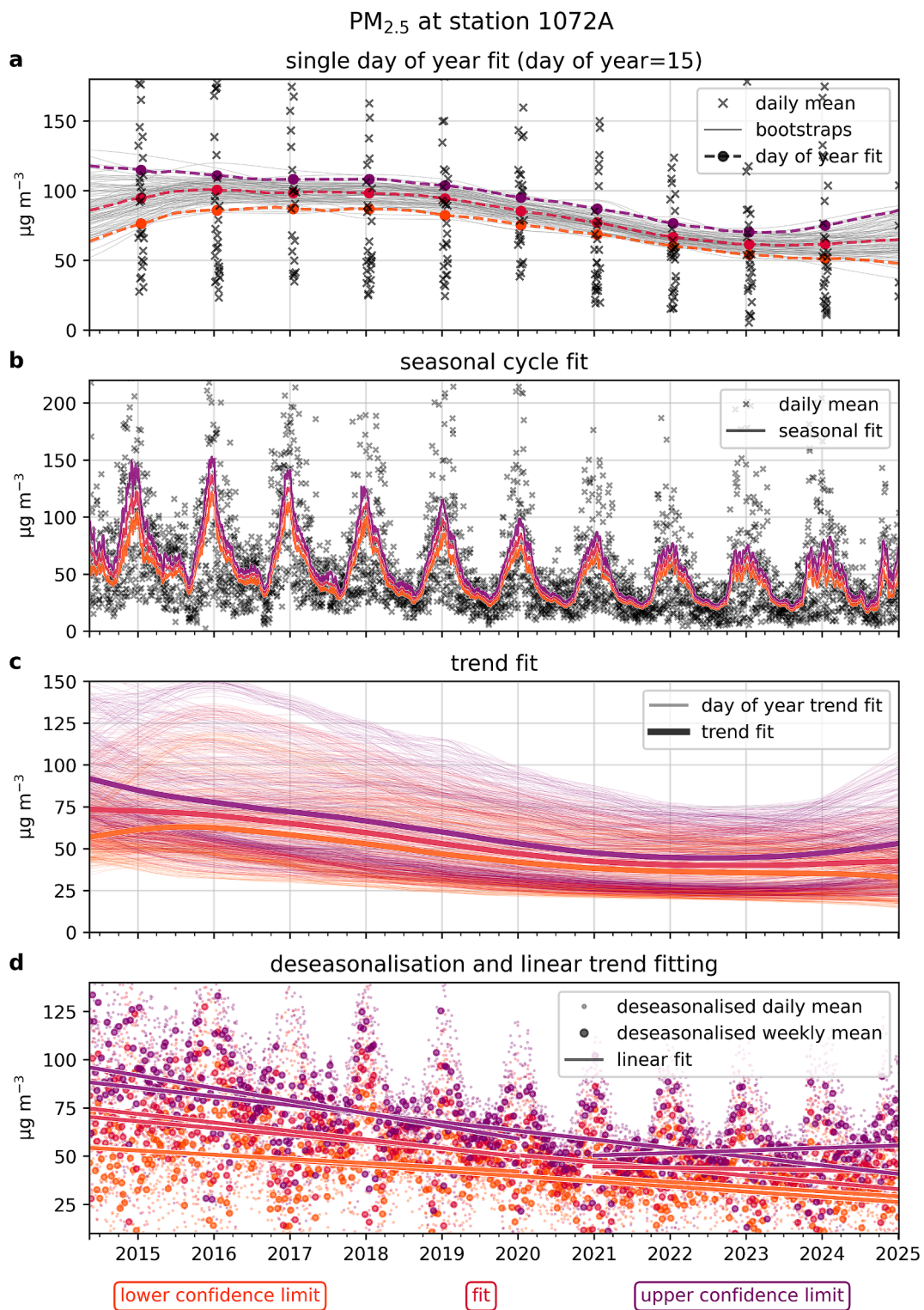
Fig. 1. Example of trend fitting on data from a single station. Original data is shown in black, the central estimates are shown in red, while the lower and upper 95% confidence intervals are shown in orange and purple, respectively. Panel (a) shows the LOWESS trend fitted for a single 'day-of-year' window, in this case is centred on the 15th day of the year, and including data during the 8th to 22nd day of the year. Panel (b) shows full seasonal cycle fit, which uses individual 'day-of-year' fits shown in (a) repeated for each day of the year. Panel (c) shows the interannual trend fit, which is the mean of the non-linear trendline calculated for each individual 'day of year' fit (i.e. in (a)). Panel (d) shows the deseasonalised data, which is calculated by subtracting the seasonal cycle in (b) and adding the trend from (c) to the daily mean data. This is used to estimate linear trends for the three periods (2015–2024, 2015–2019 and 2021–2024). (For interpretation of the references to colour in this figure legend, the reader is referred to the web version of this article.)

Futures, 2021) for future years. To ensure consistency between the GBD data and projected IF data, for the 2022–2035 mortality rates, we scale the 2021 GBD NCD and LRI mortality rates by the annual change in the IF mortality rates for NCD and total respiratory infections, respectively. To explore sensitivity to the uncertainty inherent in the input data used in the GEMM model, we propagate the uncertainties in the population data, age fractions, and the GEMM's exposure–response estimate to give 95% confidence intervals on the mortality estimates.

The health impact can either be estimated at the grid scale using gridded PM$_{2.5}$ and population count data (Conibear et al., 2022b; Geng et al., 2021; Yin, 2022) or at the country scale using regionally aggregated data, i.e. national population-weighted mean PM$_{2.5}$ and total population (Burnett et al., 2018; McDuffie et al., 2021). We henceforth term the first method, the 'gridded method,' and the second, the 'national-level method'. We use the Geographically Weighted Regression PM$_{2.5}$ reanalysis (van Donkelaar et al., 2021) to provide gridded PM$_{2.5}$ estimates, and the Gridded Population of the World (GPW) dataset (CIESIN, 2016) to provide gridded population estimates. The GPW data

provides an estimate every 5 years, and we use linear interpolation to produce annual data.

2.9. Future PM$_{2.5}$ scenarios

We generate three future PM$_{2.5}$ scenarios to demonstrate the health impact of different potential future trajectories of China's PM$_{2.5}$ concentrations. In the first scenario, "target met" we project that from the 2023 average trendline concentration of 31.6 μg m^{-3}, PM$_{2.5}$ will decrease linearly to reach the target concentration of 25 μg m^{-3} in 2035. In the second scenario, "target exceeded," PM$_{2.5}$ decreases at twice the rate of the "target met" scenario, reaching 18.4 μg m^{-3} in 2035. In the third scenario, "plateau", PM$_{2.5}$ remains at 2023 levels.

These scenarios are not intended to be realistic scenarios of future PM$_{2.5}$ trends, rather they are meant as hypothetical scenarios that are used to demonstrate the effect of plausible future PM$_{2.5}$ trends combined with demographic changes to explore the magnitude of the PM$_{2.5}$ reduction required to reduce the associated health impacts.
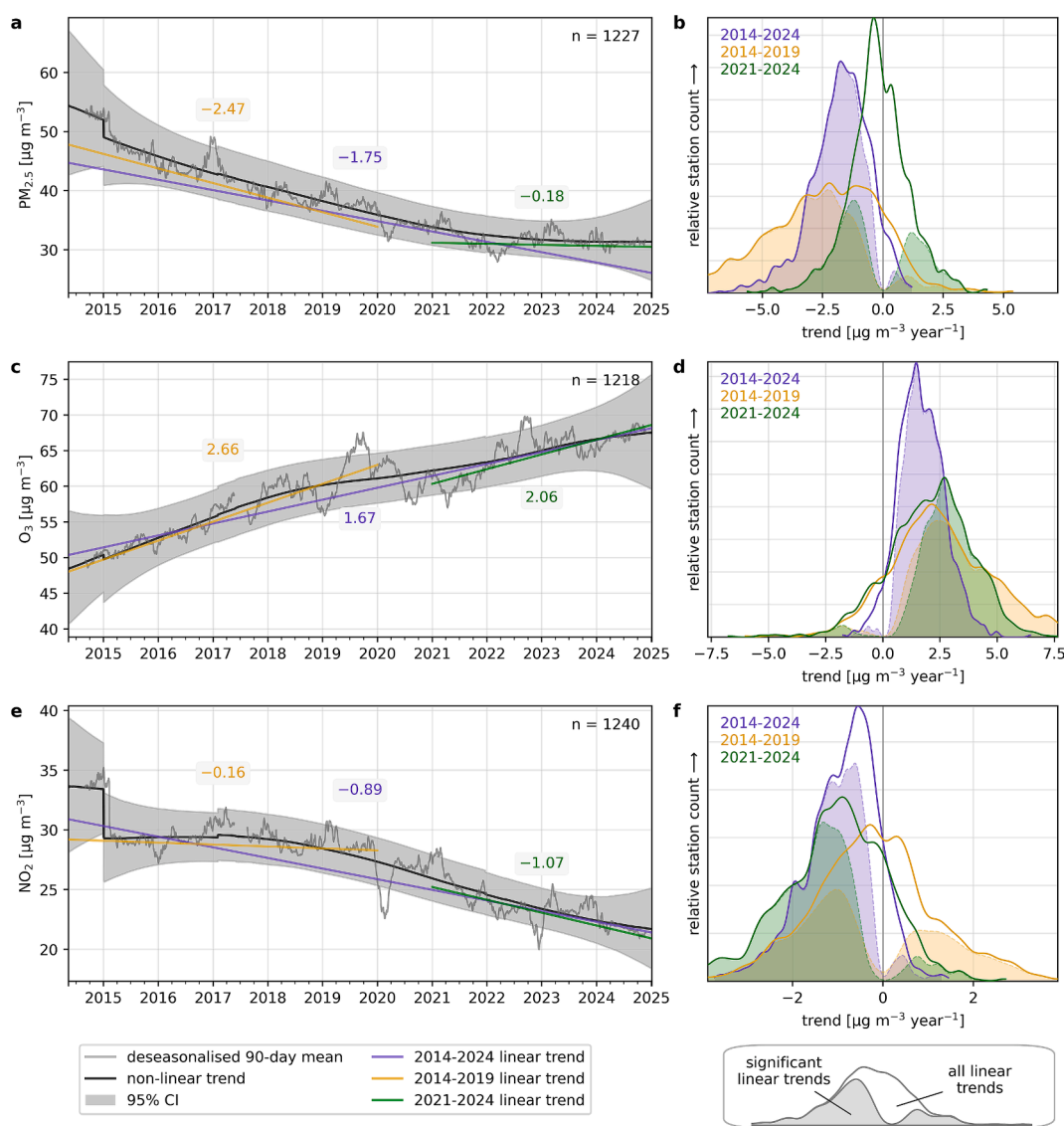
Fig. 2. Trends in PM$_{2.5}$ (a, b), ozone (c, d) and NO$_2$ (e, f) respectively. The left-hand column shows the non-linear trend during the entire period of data (black line), averaged across all the measurement stations which passed data quality checks, with the grey shaded area representing the average (across stations) 95% confidence interval. The grey line is the rolling 90-day deseasonalised mean, which is included to show variability at a shorter timescales. The straight coloured lines show the average linear trends, calculated using the Theil-Sen estimator, for three periods of interest. The numbers correspond to the average linear trend (in μg m^{-3} year^{-1}) during the period indicated by the coloured lines. The right-hand column (b, d, f) shows the frequency distribution for the linear trends during the three periods of interest across all stations meeting data quality checks. The shaded area of the frequency distribution indicates statistically significant linear trends (p < 0.05).

3. Results

3.1. Air quality trends

Our estimates of the average trend in PM$_{2.5}$ pollution measured by the CNEMC network, show that the rapid decrease in PM$_{2.5}$ concentrations that occurred during 2014–2019 has slowed in recent years (Fig. 2). The average PM$_{2.5}$ trendline concentration decreased from 49.1 µg m^{-3} with a 95% confidence interval (95CI) of 41.0 to 57.9 µg m^{-3} at the start of 2015, to 35.9 (95CI: 32.5 to 39.7) µg m^{-3} by the end of 2019. The average linear trend during this period was −2.47 (95CI: −3.09 to −1.84) µg m^{-3} year^{-1}, with 70.0% of stations having a significant negative trend. After 2020, the decrease in the trendline concentration slowed, reaching a minimum of 31.3 (95CI: 24.9 to 35.0) µg m^{-3} in March 2024. After this, the trendline concentration then plateaus, remaining at 31.3 (95CI: 24.8 to 38.5) µg m^{-3} at the end of December 2024. However, due to the wide trendline confidence intervals towards either end of the time series, there is not a statistically robust positive trend in PM$_{2.5}$. The average linear trend during January 2021-December 2024 was −0.18 (95CI: −0.51 to 0.17) µg m^{-3} year^{-1}. During this period, 15.7% of stations have a positive trend and 24.7% have a negative trend.

Fig. 3 shows that the relative rates of change in PM$_{2.5}$ trendline concentrations have been similar between the four most populated regions of China, with the average trend decreasing by >20% by 2022. In the Western China region, PM$_{2.5}$ decreases by comparatively less, only ~10%. However, it should be emphasised that the Western China region is relatively sparsely populated and has generally lower PM$_{2.5}$ concentrations than other parts of China. Average PM$_{2.5}$ concentrations fell below the World Health Organisation's (WHO) first Interim Target (IT1) of 35 µg m^{-3} during 2021–2023 in all regions except Northern East China, which is the most heavily populated and industrialised region (Supplementary Fig. 4).

In contrast with PM$_{2.5}$, ozone concentrations have been steadily increasing through the period observed by the CNEMC network (Fig. 2). The average ozone trendline concentration rose from 49.8 (95CI: 43.8 to 56.0) µg m^{-3} at the start of 2015 to 61.1 (95CI: 57.7 to 64.7) µg m^{-3} by the end of 2019. The average linear trend was 2.66 (95CI: 2.38 to 3.01) µg m^{-3} year^{-1} during this period, with 72.7% of stations having a significant positive trend. The increasing of the trendline concentration has continued in recent years, reaching 67.5 (95CI: 59.6 to 75.7) µg m^{-3} by the end of December 2024. During Jan 2021 to December 2024, the average linear trend was 2.06 (95CI: 1.41 to 2.71) µg m^{-3} year^{-1}, with 65.2% of stations having significant positive trends and 3.1% having significant negative trends.

Fig. 3 shows that during 2014–2024, the relative increase in ozone has been similar in most regions, reaching levels ~30% higher compared with 2015 levels. The exception is the Northern East China
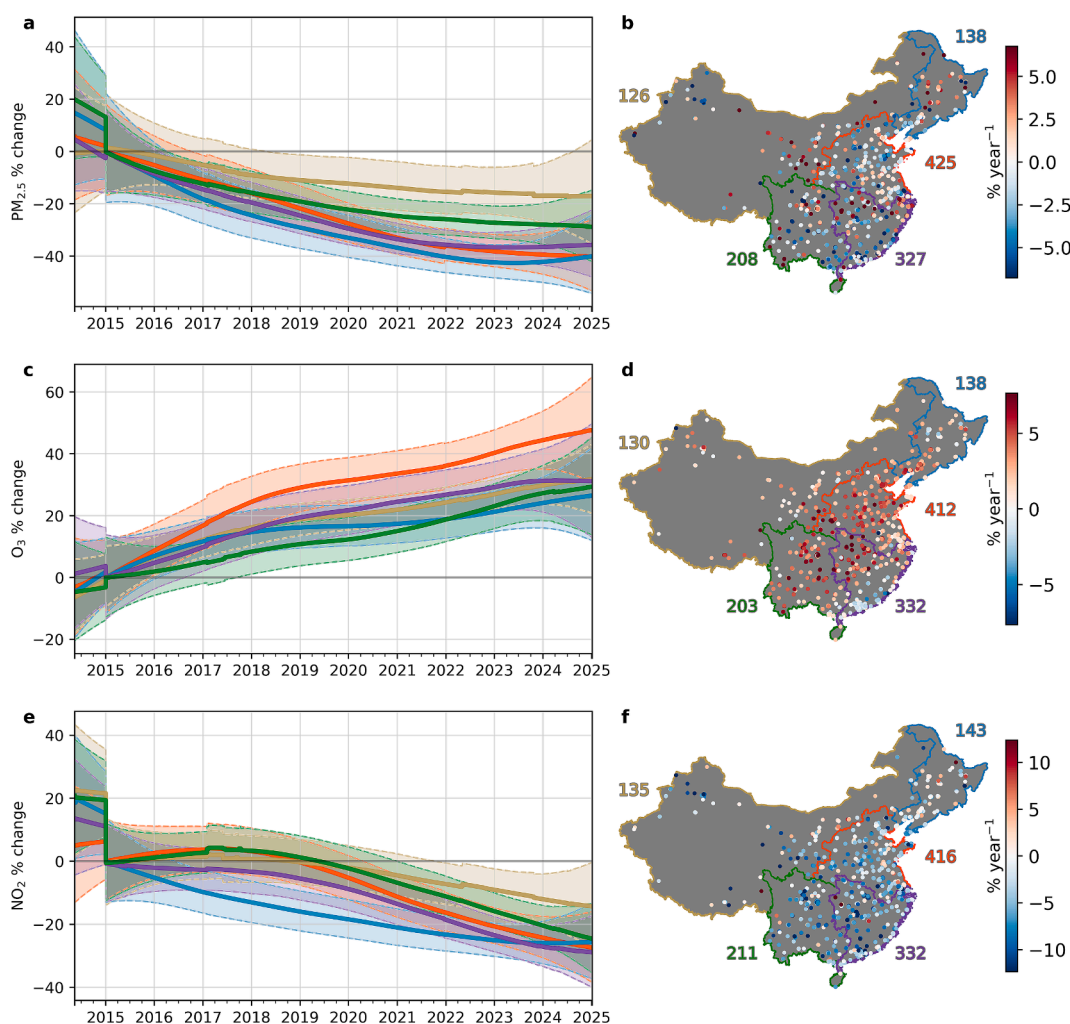
Fig. 3. Relative non-linear trends in (a, b) PM$_{2.5}$, (c, d) ozone, and (e, f) NO$_2$, averaged by region of China. In the left-hand column (a, c, e), the change is shown relative to the value at the start of 2015 (as prior to this, data from ~60% fewer stations are available). The shaded regions show the 95% confidence interval, coloured by each region. In the right-hand column (b, d, f) maps of the distribution of relative linear trends for each valid station are shown. The linear trend is calculated for the entire timeseries (2014–2024).

region, where levels have increased by >40%. In some regions, such as Southern East China, the trend in ozone appears to have flattened, however, none of the regions can be said to have peaked with >95% confidence.

NO_2 concentrations have generally fallen during the CNEMC network observation period, though the average peak concentrations generally occurred later than those of $PM_{2.5}$ (Fig. 2). During the entire time series (2014–2024), 71.7% of stations have a negative linear trend for NO_2. The overall peak in the trendline NO_2 concentration occurs in February 2017, at 29.6 (95CI: 27.4 to 33.2) µg m^{-3}. After this, the average NO_2 trendline concentration falls to 27.3 (95CI: 25.3 to 29.3) µg m^{-3} by the end of 2019, with an average linear trend of −0.16 (95CI: −0.36 to 0.07) µg m^{-3} year^{-1} during 2014–2019, with 23.2% and 34.7% of stations having significant positive and negative trends, respectively. By the end of December 2024, the average NO_2 trendline fell further to 21.7 (95CI: 18.4 to 25.1) µg m^{-3}. During 2021–2024, the average linear

trend is −1.07 (95CI: −1.18 to −0.96) µg m^{-3} year^{-1}, and 5.1% have significant positive trends and 62.1% of stations had significant negative trends. The de-seasonalised 90-day rolling mean concentration in Fig. 2e shows the clear impact of the first COVID-19 lockdowns during 2020.

The trendline in PM_{10} has a similar trajectory to $PM_{2.5}$, where there is a fast decrease in concentrations during 2014–2019, with an average linear trend of −3.44 (−4.36 to −2.52) µg m^{-3} year^{-1}, which slows during 2021 to 2024, where the average linear trend becomes −1.15 (−1.64 to −0.59) µg m^{-3} year^{-1}.

CO and SO_2 have similar overall negative trendlines in relative terms, where their rate of decrease gradually lessens and their concentrations approach relatively low levels (Supplementary Fig. 5). Their average trend does not have any statistically significant reversal in trend direction. During 2014–2019, both CO and SO_2 have steep negative trends, with significant negative linear trends at 61.2% and 84.9% of stations respectively. Both still have average negative linear trends
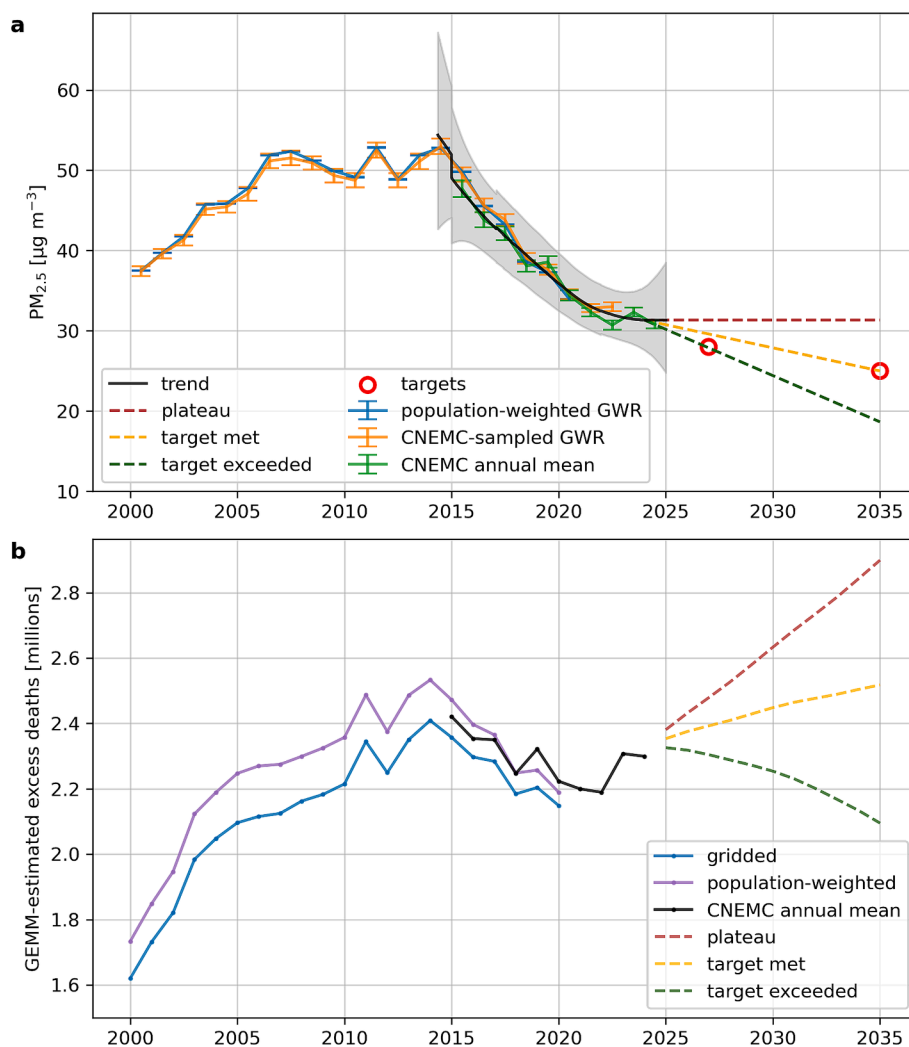
Fig. 4. Historical and future $PM_{2.5}$ concentration averages and their estimated health impacts. (a) shows the change in the mean $PM_{2.5}$ exposure across China estimated by three different methods. 'Population-weighted GWR,' uses the GWR (van Donkelaar et al., 2019) and GPW data to calculate the population-weighted mean is shown in blue. 'CNEMC-sampled GWR,' samples the GWR data at the locations of the CNEMC network and is shown in orange. 'CNEMC-annual mean' is the annual mean of all stations that pass quality control checks in the CNEMC network and is shown in green. These three lines are shown with the 95% confidence intervals of the annual means. The $PM_{2.5}$ non-linear trend and 95% confidence intervals is shown in black. $PM_{2.5}$ targets announced by the Chinese government are shown as red circles. The three hypothetical scenarios, in which $PM_{2.5}$ concentrations plateau (red), meet the 2035 target (yellow) and exceed the target (green) are shown as dotted lines. In (b), the solid lines show health impact estimations calculated from historical data, while the dotted lines show projections using the hypothetical scenarios in (a). 'Gridded' (blue) shows the health impact estimated using gridded $PM_{2.5}$ and population data, while 'population-weighted' (purple) shows the health impact estimated using a single population-weighted $PM_{2.5}$ mean, and total population value. The 'CNEMC annual mean' (black) line shows the health impact estimated using the average of the CNEMC network. The confidence intervals on the health impact estimate are shown in Supplementary Fig. 7. (For interpretation of the references to colour in this figure legend, the reader is referred to the web version of this article.)

overall during 2021–2024, but with a lower proportion of stations having significant negative trends (CO: 46.2% and SO$_2$: 43.3%), showing that the rate of decrease has slowed on average across China.

3.2. Using CNEMC network data to infer health impact

Estimates of the PM$_{2.5}$ exposure (i.e. the population-weighted mean), using solely the CNEMC network data, are similar to those derived from gridded PM$_{2.5}$ reanalysis data. Fig. 4a shows that the confidence intervals of the PM$_{2.5}$ annual means for the population-weighted (using the gridded PM$_{2.5}$ reanalysis "Geographically Weighted Regression" (GWR) product (van Donkelaar et al., 2021)) and CNEMC-sampled (sampling the gridded GWR PM$_{2.5}$ at the locations of the CNEMC network) methods overlap. This demonstrates that the CNEMC network samples PM$_{2.5}$ exposure across China's population in a stratified manner. Therefore, an average of the CNEMC network is analogous to the population-weighted mean, which can be used to calculate the health impact. Fig. 4a also shows that the annual means of the CNEMC network compare well with GWR PM$_{2.5}$ reanalysis, although they would not be expected to be an exact match due to the comparison between gridded and point data. We note that data from the CNEMC network is one of the inputs used to generate the GWR PM$_{2.5}$ reanalysis product.

In order to estimate the total PM$_{2.5}$-attributable excess mortality burden from the CNEMC network data, we show that conducting the health impact assessment using the national-level method (i.e. a single value of population-weighted PM$_{2.5}$ for the whole of China) and using the gridded method (using GWR PM$_{2.5}$ (van Donkelaar et al., 2021); Fig. 4b) both give a similar result for the total China-wide mortality burden. Supplementary Fig. 6 shows that the confidence intervals of the estimated health impacts largely overlap. The difference in the estimated excess deaths between the two methods is on average 5.6%, while the uncertainty of the excess deaths estimate itself is on average 34%. This large uncertainty is due to the propagation of uncertainty in the demographic and mortality rate data, as well as in the GEMM. Our results demonstrate that the CNEMC mean, along with future projections of population totals and demography can be used to estimate the health impact in future scenarios.

3.3. Implications for future health impact

Our estimated health impact shows that the rapid decrease in population-weighted PM$_{2.5}$, which began around 2015, has resulted in modest reductions in PM$_{2.5}$-attributed excess deaths (Fig. 4). Prior to 2015, before the CNEMC observation period, we estimate the health impact using GWR data. During 2000 to 2008, population-weighted PM$_{2.5}$ increases from less than 40 μg m^{-3} to around 50 μg m^{-3}. The estimated PM$_{2.5}$-attributable mortality burden also increases, from 1.62 (95CI: 1.38 to 1.87) million excess deaths per year to 2.16 (95CI: 1.86 to 2.50) million. During 2008–2014, the population-weighted PM$_{2.5}$ fluctuates between 49 and 53 μg m^{-3}, while the excess deaths continue to steadily increase, reaching 2.41 (95CI: 2.02 to 2.86) million per year by 2014. From 2015, the rapid decrease in population-weighted PM$_{2.5}$ begins, falling from ~50 μg m^{-3} to < 35 μg m^{-3} by 2020. As the rate in the decrease of population-weighted PM$_{2.5}$ slows, it gradually becomes insufficient to outweigh the increases in the associated mortality burden driven by demographic factors, resulting in estimated deaths no longer clearly decreasing post-2020.

Our hypothetical future scenarios demonstrate that continuing to alleviate the health impact from PM$_{2.5}$ will become challenging in China, due to its growing and ageing population (Supplementary Fig. 7). Our mid-range scenario, 'target met,' shows that even if China meets its target of reaching average PM$_{2.5}$ concentrations of 25 μg m^{-3} by 2035, PM$_{2.5}$-attributed excess deaths will again start to increase, reaching 2.52 (95CI: 1.82 to 3.35) million annual excess deaths by 2035.

To decrease the total mortality burden attributable to PM$_{2.5}$ during the next decade, population-weighted concentrations would need to decrease at twice the rate as in the "target met" scenario, as shown in the "target exceeded" scenario. In this scenario, the rapid decrease in PM$_{2.5}$ observed during 2015–2020 would need to be resumed, which would result in the mortality burden falling to 2.10 (95CI: 1.52 to 2.79) million annual excess deaths. Our trend analysis finds that the rate of PM$_{2.5}$ decrease has slowed, and possibly even plateaued during recent years. Our "plateau" scenario demonstrates what would happen if PM$_{2.5}$ remained at 2024 levels until 2035. In this scenario, the PM$_{2.5}$-attributable mortality burden increases rapidly, reaching 2.90 (95CI: 2.10 to 3.85) million annual excess deaths in 2035.

The key driver behind the predicted increase in excess deaths is the ageing population (Supplementary Fig. 7a). While underlying non-communicable disease and respiratory infection mortality rates are projected to fall in every age group as China's healthcare systems improve, as the population ages, older age groups become relatively larger. As adult mortality rates of non-communicable diseases and lower respiratory infections increase exponentially with age (Supplementary Fig. 7b), ageing results in the population-average mortality rate increasing rapidly (Supplementary Fig. 7c).

4. Discussion

Our analysis shows that the rapid decrease in PM$_{2.5}$ concentrations in China observed during 2014–2019 has slowed during 2021–2024. PM$_{2.5}$-attributed deaths have been declining in China prior to 2020 (Li et al., 2023), due to the sustained reduction in exposure, along with an improvement in underlying health, which has compensated for the increasing population size and average age (Geng et al., 2021; Li et al., 2023). We found that during recent years, the slowing rate of PM$_{2.5}$ decrease as well as demographic changes have halted the decline in the mortality burden. Furthermore, even if PM$_{2.5}$ concentrations further decline to reach the target of an average concentration of 25 μg m^{-3} by 2035, this will not be enough to prevent the total health impact of PM$_{2.5}$ worsening in China. We show that a PM$_{2.5}$ reduction target around twice as ambitious would be needed to offset the impact of demographic changes and alleviate the excess deaths due to PM$_{2.5}$ exposure. The difficulty in reducing excess deaths is primary due to the rapidly ageing population, as population growth is slowing, and underlying mortality rates are decreasing (Xu et al., 2023). This further highlights the need for China to sustain air quality improvement, as it may be the only way to alleviate impacts resulting from future demographic change.

China has made remarkably rapid progress and has achieved the WHO's IT1 of 35 μg m^{-3}, which we estimate occurred during 2020. The average PM$_{2.5}$ concentration fell by 17 μg m^{-3} over 8 years, to reach 32 μg m^{-3} in 2022. China has recently announced it will aim for the WHO's IT2 of 25 μg m^{-3}, by 2035 (Reuters, 2024). As of 2024, PM$_{2.5}$ concentrations have reached 31 μg m^{-3}. This leaves more than 10 years to achieve a further reduction of ~7 μg m^{-3}, or a ~2.3% reduction per year (based on 2024 levels). During 2014–2024, China reduced PM$_{2.5}$ by ~5.1% year^{-1}. Given the Chinese government prefers to under-promise and over-deliver (Green and Stern, 2017), this shows that it remains committed to rapidly improving air quality. The WHO's new Air Quality Guideline (AQG) for PM$_{2.5}$ is 5 μg m^{-3}, based on a review of epidemiological evidence which suggests negative health impacts from PM$_{2.5}$ exposure can occur even at this relatively low level (World Health Organization, 2021). Meeting this target will be challenging for many regions of the world (Pai et al., 2022; Reddington et al., 2023). If similar rates of decrease that occurred after the implementation of the Action Plan during 2014–2019 were maintained, it would take China ~40 years to achieve, and require policies targeted at emission sectors that have so far not seen large reductions (Conibear et al., 2022a).

Our analysis suggests that it is unlikely that ozone concentrations have peaked. According to Li et al. (2019), the main driver of the ozone increase during 2013–2017 was the decrease in HO$_2$ radical uptake onto aerosol, driven by the decrease in PM$_{2.5}$. They suggest that without any change in aerosols, ozone levels would have fallen due to NO$_x$ and VOC

emissions changes. However, during 2020–2024, the rate of PM$_{2.5}$ increase has slowed, while ozone levels have continued to increase, suggesting that aerosol concentrations have not been a major driver of ozone change during this period. According to Wang et al. (2023), ozone levels had become much less sensitive to aerosol concentrations by 2021. However, Wang et al. (2023) estimate that ozone concentrations were falling during 2018–2021, when adjusting for the effect of meteorological variability. Our analysis shows this was not the case, which suggests model simulations may struggle to accurately capture the trend in ozone. Future research should use state-of-the-art atmospheric chemistry models to understand the complex interactions between PM$_{2.5}$ and ozone to accurately identify drivers of ozone increases and identify pathways for simultaneous PM$_{2.5}$ and ozone reduction.

Our analysis confirms the steep reductions in NO$_2$ concentrations that were observed immediately after the first wave of COVID-19 lockdowns (Silver et al., 2020; Wang et al., 2021). NO$_2$ concentrations quickly recovered by mid-2020, then continued to fall at a rate similar to the pre-lockdown trend.

The potential peak in ozone coincides with periods of increase in PM$_{2.5}$ and NO$_x$ (indicated by NO$_2$), which under NO$_x$-saturated conditions both have the potential to decrease ozone levels, via HO$_2$ uptake and NO titration respectively. However, PM$_{2.5}$ and NO$_2$ concentrations can be expected to eventually fall, as China's air quality control efforts continue, and further shifts in the balance between NO$_x$ and VOC emissions may change the prevalence of NO$_x$-saturated conditions. This makes it difficult to conclude to what extent the observed falls in ozone will be sustained, and how ozone may respond to future changes in NO$_x$ and PM$_{2.5}$. Further modelling studies are needed to disentangle the relationship between ozone, aerosol concentrations, and NO$_x$ emissions during the complex lockdown and economic recovery period.

The difficulty of accessing China's network data is a significant barrier to enabling research by the global scientific community. The non-governmental organisation OpenAQ, whose mission is to aggregate, harmonise and release the world's air quality data, defines four key criteria for government's monitoring network data to be considered 'fully open' (Sawant et al., 2022). Currently, China only meets two of the criteria, as it does not provide programmatic access to historical data, or a list or monitoring station coordinates, while it does share data in near-real time, and using physical units. We hope that releasing the observations of the CNEMC network thus-far, in an easily accessible format and with data quality flags, will facilitate improved access to these important data. We also recognise that there is still a need for official metadata and documentation, which we hope will be released by the CNEMC to improve access for researchers outside China.

5. Conclusion

Our analysis of China's air quality network data shows that in recent years air quality trends in China appear to have entered a new paradigm. During 2014–2019, trends in China's air quality were characterised by a rapid decrease in PM$_{2.5}$ concentrations, resulting in improved air quality across much of the country. Furthermore, concentrations of NO$_2$, SO$_2$ and CO have all continued to fall up to 2024, suggesting widespread decreases in emissions. During 2020–2024, the decrease in PM$_{2.5}$ has slowed, which if sustained has the potential to worsen the air pollution health burden in China over the coming years, particularly given its ageing population. At the same time, ozone concentrations have continually increased, which previous studies suggest is an unintended consequence of China's air quality control policies rather than being driven by increases in emissions. However, due to the health impacts of PM$_{2.5}$ being an order of magnitude larger than those of ozone, air quality control policies have still resulted in a net-benefit in terms of air pollution health impacts. A PM$_{2.5}$ target around twice as ambitious as is currently in place would be needed to peak the increase in PM$_{2.5}$-attributed excess deaths by 2035. A limitation of our study is that we do not have access to more granular (e.g. provincial level) demographic

projections, which would allow regional differences in health outcomes and population ageing in China to be taken into account to produce more accurate air quality health impact estimates.

Further research is needed to untangle the complex relationship between changes in ozone, NO$_x$ and PM$_{2.5}$, and to assess the extent to which changes in emissions due to the COVID-19 pandemic, and its long-term effects, have impacted air quality. Furthermore, China's recent economic trajectory can be expected to alter future anthropogenic emissions projections. Future trends in China's air quality should continue to be closely monitored to understand whether the recent apparent slowdown in improvement during the last four years is a temporary pause or a new paradigm. Further work could use atmospheric chemistry modelling to explore the emissions reductions policies that would be needed to achieve the PM$_{2.5}$ decrease we have demonstrated is necessary to resume reduction of the air quality health impact.

Data and code availability

The CNEMC monitoring data is available in an easy-to-use format from the Figshare repository (https://doi.org/10.6084/m9.figshare.25689477). This includes the raw data, data adjusted for the protocol change (see Methods) and data with outliers removed using the PAOD algorithm. The repository also includes Python scripts to perform the analysis, including the PAOD algorithm and the non-linear trend extraction. The data and code needed to reproduce all figures is also included in the repository.

CRediT authorship contribution statement

Ben Silver: Writing – review & editing, Writing – original draft, Visualization, Validation, Software, Methodology, Investigation, Formal analysis, Data curation, Conceptualization. **Carly L. Reddington:** Writing – review & editing, Writing – original draft, Supervision, Methodology, Conceptualization. **Yue Chen:** Writing – review & editing, Data curation. **Steve R. Arnold:** Writing – review & editing, Writing – original draft, Supervision, Methodology, Investigation, Funding acquisition, Conceptualization.

Declaration of competing interest

The authors declare that they have no known competing financial interests or personal relationships that could have appeared to influence the work reported in this paper.

Appendix A. Supplementary data

Supplementary data to this article can be found online at https://doi.

org/10.1016/j.envint.2025.109318.

References

Andrews, S.Q., 2008. Inconsistencies in air quality metrics: "Blue Sky" days and PM10 concentrations in Beijing. Environ. Res. Lett. 3, 034009. https://doi.org/10.1088/1748-9326/3/3/034009.

Beyer, S., 2006. Environmental Law and Policy in the People's Republic of China. Chin. J. Int. Law 5, 185–211. https://doi.org/10.1093/chinesejil/jmk002.

Brimblecombe, P., Zong, H., 2019. Citizen perception of APEC blue and air pollution management. Atmos. Environ. 214, 116853. https://doi.org/10.1016/j.atmosenv.2019.116853.

Burnett, R., Chen, H., Szyszkowicz, M., Fann, N., Hubbell, B., Pope, C.A., Apte, J.S., Brauer, M., Cohen, A., Weichenthal, S., Coggins, J., Di, Q., Brunekreef, B., Frostad, J., Lim, S.S., Kan, H., Walker, K.D., Thurston, G.D., Hayes, R.B., Lim, C.C., Turner, M.C., Jerrett, M., Krewski, D., Gapstur, S.M., Diver, W.R., Ostro, B., Goldberg, D., Crouse, D.L., Martin, R.V., Peters, P., Pinault, L., Tjepkema, M., Van Donkelaar, A., Villeneuve, P.J., Miller, A.B., Yin, P., Zhou, M., Wang, L., Janssen, N. A.H., Marra, M., Atkinson, R.W., Tsang, H., Thach, T.Q., Cannon, J.B., Allen, R.T., Hart, J.E., Laden, F., Cesaroni, G., Forastiere, F., Weinmayr, G., Jaensch, A., Nagel, G., Concin, H., Spadaro, J.V., 2018. Global estimates of mortality associated with longterm exposure to outdoor fine particulate matter. Proc. Natl. Acad. Sci. u. s. a. 115, 9592–9597. https://doi.org/10.1073/pnas.1803222115.

Center for International Earth Science Information Network - CIESIN - Columbia University, 2016. Gridded Population of the World, Version 4 (GPWv4): Population Count.

Chai, J., Hao, Y., Wu, H., Yang, Y., 2021. Do constraints created by economic growth targets benefit sustainable development? Evidence from China. Bus. Strategy Environ. 30, 4188–4205. https://doi.org/10.1002/bse.2864.

Chang, K.-L., Petropavlovskikh, I., Copper, O.R., Schultz, M.G., Wang, T., 2017. Regional trend analysis of surface ozone observations from monitoring networks in eastern North America, Europe and East Asia. Elem Sci Anth 5, 50. https://doi.org/10.1525/elementa.243.

Cleveland, W.S., 1979. Robust locally weighted regression and smoothing scatterplots. J. Am. Stat. Assoc. https://doi.org/10.1080/01621459.1979.10481038.

Cleveland, R.B., Cleveland, W.S., McRae, J.E., Terpenning, I., et al., 1990. STL: A seasonal-trend decomposition. J Stat 6, 3–73.

Conibear, L., Reddington, C.L., Silver, B.J., Arnold, S.R., Turnock, S.T., Klimont, Z., Spracklen, D.V., 2022a. The contribution of emission sources to the future air pollution disease burden in China. Environ. Res. Lett. 17, 064027. https://doi.org/10.1088/1748-9326/ac6f6f.

Conibear, L., Reddington, C.L., Silver, B.J., Chen, Y., Arnold, S.R., Spracklen, D.V., 2022b. Emission Sector Impacts on Air Quality and Public Health in China From 2010 to 2020. GeoHealth 6, e2021GH000567. https://doi.org/10.1029/2021GH000567.

Dyson, J.E., Whalley, L.K., Slater, E.J., Woodward-Massey, R., Ye, C., Lee, J.D., Squires, F., Hopkins, J.R., Dunmore, R.E., Shaw, M., Hamilton, J.F., Lewis, A.C., Worrall, S.D., Bacak, A., Mehra, A., Bannan, T.J., Coe, H., Percival, C.J., Ouyang, B., Hewitt, C.N., Jones, R.L., Crilley, L.R., Kramer, L.J., Acton, W.J.F., Bloss, W.J., Saksakulkrai, S., Xu, J., Shi, Z., Harrison, R.M., Kotthaus, S., Grimmond, S., Sun, Y., Xu, W., Yue, S., Wei, L., Fu, P., Wang, X., Arnold, S.R., Heard, D.E., 2023. Impact of HO_2 aerosol uptake on radical levels and O_3 production during summertime in Beijing. Atmospheric Chem. Phys. 23, 5679–5697. https://doi.org/10.5194/acp-23-5679-2023.

Ferreri, J.M., Peng, R.D., Bell, M.L., Ya, L., Li, T., Brooke Anderson, G., 2018. The January 2013 Beijing "Airpocalypse" and its acute effects on emergency and outpatient visits at a Beijing hospital. Air Qual. Atmosphere Health 11, 301–309. https://doi.org/10.1007/s11869-017-0538-0.

Florig, H.K., Sun, G., Song, G., 2002. Evolution of particulate regulation in China - Prospects and challenges of exposure-based control. Chemosphere 49, 1163–1174. https://doi.org/10.1016/S0045-6535(02)00246-1.

Frederick S. Pardee Center for International Futures, 2021. International Futures (IFs) modeling system. Version 8.06.

Geng, G., Zheng, Y., Zhang, Q., Xue, T., Zhao, H., Tong, D., Zheng, B., Li, M., Liu, F., Hong, C., He, K., Davis, S.J., 2021. Drivers of PM2.5 air pollution deaths in China 2002–2017. Nat. Geosci. 14, 645–650. https://doi.org/10.1038/s41561-021-00792-3.

Ghanem, D., Zhang, J., 2014. "Effortless Perfection:" Do Chinese cities manipulate air pollution data? J. Environ. Econ. Manag. 68, 203–225. https://doi.org/10.1016/j.jeem.2014.05.003.

Global Burden of Disease Collaborative Network, 2024. Global Burden of Disease Study 2021. Institute for Health Metrics and Evaluation (IHME), Seattle, WA.

Green, F., Stern, N., 2017. China's changing economy: implications for its carbon dioxide emissions. Clim. Policy 17, 423–442. https://doi.org/10.1080/14693062.2016.1156515.

Hamed, K.H., Rao, A. Ramachandra, 1998. A modified Mann-Kendall trend test for autocorrelated data. J. Hydrol. 204, 182–196. https://doi.org/10.1016/S0022-1694(97)00125-X.

Han, L., Zhou, W., Li, W., 2015. City as a major source area of fine particulate ($PM_{2.5}$) in China. Environ. Pollut. 206, 183–187. https://doi.org/10.1016/j.envpol.2015.06.038.

Hao, J., Wang, S., Liu, B., He, K., 2001. Plotting of acid rain and sulfur dioxide pollution control zones and integrated control planning in China. Water. Air. Soil Pollut. 130, 259–264. https://doi.org/10.1023/A:1013823505195.

He, Q., Gao, K., Zhang, L., Song, Y., Zhang, M., 2021. Satellite-derived 1-km estimates and long-term trends of PM2.5 concentrations in China. Environ. Int. 156, 106726. https://doi.org/10.1016/j.envint.2021.106726 from 2000 to 2018.

He, G., Pan, Y., Tanaka, T., 2020. The short-term impacts of COVID-19 lockdown on urban air pollution in China. Nat. Sustain. 3, 1005–1011. https://doi.org/10.1038/s41893-020-0581-y.

Hersbach, H., Bell, B., Berrisford, P., Hirahara, S., Horányi, A., Muñoz-Sabater, J., Nicolas, J., Peubey, C., Radu, R., Schepers, D., Simmons, A., Soci, C., Abdalla, S., Abellan, X., Balsamo, G., Bechtold, P., Biavati, G., Bidlot, J., Bonavita, M., Chiara, G., Dahlgren, P., Dee, D., Diamantakis, M., Dragani, R., Flemming, J., Forbes, R., Fuentes, M., Geer, A., Haimberger, L., Healy, S., Hogan, R.J., Hólm, E., Janisková, M., Keeley, S., Laloyaux, P., Lopez, P., Lupu, C., Radnoti, G., Rosnay, P., Rozum, I., Vamborg, F., Villaume, S., Thépaut, J., 2020. The ERA5 global reanalysis. Q. J. r. Meteorol. Soc. 146, 1999–2049. https://doi.org/10.1002/qj.3803.

Huang, R., Zhang, Y., Bozzetti, C., Ho, K.F., Cao, J.J., Han, Y., Daellenbach, K.R., Slowik, J.G., Platt, S.M., Canonaco, F., Zotter, P., Wolf, R., Pieber, S.M., Bruns, E.A., Crippa, M., Ciarelli, G., Piazzalunga, A., Schwikowski, M., Abbaszade, G., Schnelle-Kreis, J., Zimmermann, R., An, Z., Szidat, S., Baltensperger, U., El Haddad, I., Prévôt, A.S.H., 2015. High secondary aerosol contribution to particulate pollution during haze events in China. Nature 514, 218–222. https://doi.org/10.1038/nature13774.

Hussain, Md., Mahmud, I., 2019. pyMannKendall: a python package for non parametric Mann Kendall family of trend tests. J. Open Source Softw. 4, 1556. https://doi.org/10.21105/joss.01556.

Institute for Health Metrics and Evaluation (IHME), 2020. Global Fertility, Mortality, Migration, and Population Forecasts 2017-2100. Seattle, United States of America: Institute for Health Metrics and Evaluation (IHME). https://doi.org/10.6069/MJND-3671.

Ivatt, P.D., Evans, M.J., Lewis, A.C., 2022. Suppression of surface ozone by an aerosol-inhibited photochemical ozone regime. Nat. Geosci. 15, 536–540. https://doi.org/10.1038/s41561-022-00972-9.

Jiang, S., Lin, X., Qi, L., Zhang, Y., Sharp, B., 2022. The macro-economic and CO2 emissions impacts of COVID-19 and recovery policies in China. Econ. Anal. Policy 76, 981–996. https://doi.org/10.1016/j.eap.2022.10.008.

Jin, Y., Andersson, H., Zhang, S., 2016. Air pollution control policies in China: A retrospective and prospects. Int. J. Environ. Res. Public. Health 13. https://doi.org/10.3390/ijerph13121219.

Jin, L., Zhang, J.J., Ma, X., Connaughton, D.P., 2011. Residents' Perceptions of Environmental Impacts of the 2008 Beijing Green Olympic Games. Eur. Sport Manag. q. 11, 275–300. https://doi.org/10.1080/16184742.2011.577791.

Jin, L., Wang, B., Shi, G., Seyler, B.C., Qiao, X., Deng, X., Jiang, X., Yang, F., Zhan, Y., 2020. Impact of china's recent amendments to air quality monitoring protocol on reported trends. Atmosphere 11, 1199. https://doi.org/10.3390/atmos11111199.

Kong, L., Tang, X., Zhu, J., Wang, Z., Li, J., Wu, H., Wu, Q., Chen, H., Zhu, L., Wang, W., Liu, B., Wang, Q., Chen, D., Pan, Y., Song, T., Li, F., Zheng, H., Jia, G., Lu, M., Wu, L., Carmichael, G.R., 2021. A 6-year-long (2013-2018) high-resolution air quality reanalysis dataset in China based on the assimilation of surface observations from CNEMC. Earth Syst. Sci. Data 13, 529–570. https://doi.org/10.5194/essd-13-529-2021.

Krotkov, N.A., McLinden, C.A., Li, C., Lamsal, L.N., Celarier, E.A., Marchenko, S.V., Swartz, W.H., Bucsela, E.J., Joiner, J., Duncan, B.N., Folkert Boersma, K., Pepijn Veefkind, J., Levelt, P.F., Fioletov, V.E., Dickerson, R.R., He, H., Lu, Z., Streets, D.G., 2016. Aura OMI observations of regional SO2 and NO2 pollution changes from 2005 to 2015. Atmospheric Chem. Phys. 16, 4605–4629. https://doi.org/10.5194/acp-16-4605-2016.

Li, S., Gao, Y., Zhang, J., Hong, C., Zhang, S., Chen, D., Wild, O., Feng, Z., Xu, Y., Guo, X., Kou, W., Yan, F., Ma, M., Yao, X., Gao, H., Davis, S.J., 2024. Mitigating climate change and ozone pollution will improve Chinese food security. One Earth. https://doi.org/10.1016/j.oneear.2024.12.002.

Li, K., Jacob, D.J., Liao, H., Shen, L., Zhang, Q., Bates, K.H., 2019. Anthropogenic drivers of 2013–2017 trends in summer surface ozone in China. Proc. Natl. Acad. Sci. u. s. a. https://doi.org/10.1073/pnas.1812168116.

Li, J., Li, C., Zhao, C., Su, T., 2016. Changes in surface aerosol extinction trends over China during 1980–2013 inferred from quality-controlled visibility data. Geophys. Res. Lett. 43, 8713–8719. https://doi.org/10.1002/2016GL070201.

Li, C., van Donkelaar, A., Hammer, M.S., McDuffie, E.E., Burnett, R.T., Spadaro, J.V., Chatterjee, D., Cohen, A.J., Apte, J.S., Southerland, V.A., Anenberg, S.C., Brauer, M., Martin, R.V., 2023. Reversal of trends in global fine particulate matter air pollution. Nat. Commun. 14, 5349. https://doi.org/10.1038/s41467-023-41086-z.

Li, H., Zheng, B., 2023. TROPOMI NO2 Shows a Fast Recovery of China's Economy in the First Quarter of 2023. Environ. Sci. Technol. Lett. 10, 635–641. https://doi.org/10.1021/acs.estlett.3c00386.

Lin, M., Fiore, A.M., Horowitz, L.W., Cooper, O.R., Naik, V., Holloway, J., Johnson, B.J., Middlebrook, A.M., Oltmans, S.J., Pollack, I.B., Ryerson, T.B., Warner, J.X., Wiedinmyer, C., Wilson, J., Wyman, B., 2012. Transport of Asian ozone pollution into surface air over the western United States in spring. J. Geophys. Res. Atmospheres 117. https://doi.org/10.1029/2011JD016961.

Liu, M., Matsui, H., 2021. Aerosol radiative forcings induced by substantial changes in anthropogenic emissions in China from 2008 to 2016. Atmospheric Chem. Phys. 21, 5965–5982. https://doi.org/10.5194/acp-21-5965-2021.

Liu, W., Wang, T., 2020. Worsening urban ozone pollution in China from 2013 to 2017 - Part 2: The effects of emission changes and implications for multi-pollutant control. Atmospheric Chem. Phys. 20, 6323–6337. https://doi.org/10.5194/acp-20-6323-2020.

Liu, Y., Geng, G., Cheng, J., Liu, Y., Xiao, Q., Liu, L., Shi, Q., Tong, D., He, K., Zhang, Q., 2023. Drivers of Increasing Ozone during the Two Phases of Clean Air Actions in

China 2013–2020. Environ. Sci. Technol. 57, 8954–8964. https://doi.org/10.1021/acs.est.3c00054.

Lu, S., Chen, W., Li, X., Zheng, P., 2018. The Chinese Smog Crisis as Media Event: Examining Twitter Discussion of the Documentary Under the Dome. Policy Internet 10, 483–508. https://doi.org/10.1002/poi3.191.

Lu, Z., Streets, D.G., Zhang, Q., Wang, S., Carmichael, G.R., Cheng, Y.F., Wei, C., Chin, M., Diehl, T., Tan, Q., 2010. Sulfur dioxide emissions in China and sulfur trends in East Asia since 2000. Atmospheric Chem. Phys. 10, 6311–6331. https://doi.org/10.5194/acp-10-6311-2010.

Lu, X.i., Zhang, S., Xing, J., Wang, Y., Chen, W., Ding, D., Wu, Y., Wang, S., Duan, L., Hao, J., 2020. Progress of Air Pollution Control in China and Its Challenges and Opportunities in the Ecological Civilization Era. Engineering 6, 1423–1431. https://doi.org/10.1016/j.eng.2020.03.014.

Lu, X., Zhang, L., Wang, X., Gao, M., Li, K., Zhang, Y., Yue, X., Zhang, Y., 2020. Rapid Increases in Warm-Season Surface Ozone and Resulting Health Impact in China since 2013. Environ. Sci. Technol. Lett. 7, 240–247. https://doi.org/10.1021/acs.estlett.0c00171.

Luo, H., Tang, X., Wu, H., Kong, L., Wu, Q., Cao, K., Song, Y., Luo, X., Wang, Y., Zhu, J., Wang, Z., 2022. The Impact of the Numbers of Monitoring Stations on the National and Regional Air Quality Assessment in China During 2013–18. Adv. Atmospheric Sci. 39, 1709–1720. https://doi.org/10.1007/s00376-022-1346-5.

Ma, Z., Xu, J., Quan, W., Zhang, Z., Lin, W., Xu, X., 2016. Significant increase of surface ozone at a rural site, north of eastern China. Atmospheric Chem. Phys. 16, 3969–3977. https://doi.org/10.5194/acp-16-3969-2016.

Ma, Z., Liu, R., Liu, Y., Bi, J., 2019. Effects of air pollution control policies on PM 2.5 pollution improvement in China from 2005 to 2017: A satellite-based perspective. Atmospheric Chem. Phys. 19, 6861–6877. https://doi.org/10.5194/acp-19-6861-2019.

McDuffie, E., Martin, R., Yin, H., Brauer, M., 2021. Global Burden of Disease from Major Air Pollution Sources (GBD MAPS): A Global Approach. Res. Rep. Health Eff. Inst. 2021, 210.

Organization, W.H., et al., 2021. WHO global air quality guidelines: particulate matter (PM$_{2.5}$ and PM$_{10}$), ozone, nitrogen dioxide, sulfur dioxide and carbon monoxide. World Health Organization.

Pai, S.J., Carter, T.S., Heald, C.L., Kroll, J.H., 2022. Updated World Health Organization Air Quality Guidelines Highlight the Importance of Non-anthropogenic PM2.5. Environ. Sci. Technol. Lett. 9, 501–506. https://doi.org/10.1021/acs.estlett.2c00203.

Peng, J., Chen, S., Lü, H., Liu, Y., Wu, J., 2016. Spatiotemporal patterns of remotely sensed PM2.5concentration in China from 1999 to 2011. Remote Sens. Environ. 174, 109–121. https://doi.org/10.1016/j.rse.2015.12.008.

Qu, R., Han, G., 2021. A critical review of the variation in rainwater acidity in 24 Chinese cities during 1982–2018. Elem. Sci. Anthr. 9. https://doi.org/10.1525/elementa.2021.00142.

Ravetti, C., Swanson, T., Jin, Y., Mu, Q., Zhang, S., 2019. A dragon eating its own tail: public control of air pollution information in China. Environ. Dev. Econ. 24, 1–22. https://doi.org/10.1017/S1355770X18000414.

Reddington, C.L., Turnock, S.T., Conibear, L., Forster, P.M., Lowe, J.A., Ford, L.B., Weaver, C., van Bavel, B., Dong, H., Alizadeh, M.R., Arnold, S.R., 2023. Inequalities in Air Pollution Exposure and Attributable Mortality in a Low Carbon Future. Earths. Future 11, e2023EF003697. https://doi.org/10.1029/2023EF003697.

Reuters, 2024. China proposes new target for better air quality. Reuters. https://www.reuters.com/world/china/china-adjusts-2027-2035-targets-better-air-quality-2024-01-11/.

Rohde, R.A., Muller, R.A., 2015. Air pollution in China: Mapping of concentrations and sources. PLoS ONE 10, e0135749. https://doi.org/10.1371/journal.pone.0135749.

Sawant, V., Hagerbaumer, C., Rosales, C.M.F., Isied, M., Biggs, R., 2022. 2022 Open Air Quality Data: The Global Landscape.

Schreifels, J.J., Fu, Y., Wilson, E.J., 2012. Sulfur dioxide control in China: Policy evolution during the 10th and 11th Five-year Plans and lessons for the future. Energy Policy 48, 779–789. https://doi.org/10.1016/j.enpol.2012.06.015.

Seabold, S., Perktold, J., 2010. Statsmodels: Econometric and Statistical Modeling with Python. PROC 9th PYTHON Sci. CONF.

Sen, P.K., 1968. Estimates of the Regression Coefficient Based on Kendall's Tau. J. Am. Stat. Assoc. 63, 1379–1389. https://doi.org/10.1080/01621459.1968.10480934.

Shi, W., Bi, J., Liu, R., Liu, M., Ma, Z., 2021. Decrease in the chronic health effects from PM$_{2.5}$ during the 13th Five-Year Plan in China: Impacts of air pollution control policies. J. Clean. Prod. 317, 128433. https://doi.org/10.1016/j.jclepro.2021.128433.

Silver, B.J., 2021. Air quality in China: Trends, drivers and mitigation. University of Leeds. https://etheses.whiterose.ac.uk/id/eprint/29738/.

Silver, B., Reddington, C.L., Arnold, S.R., Spracklen, D.V., 2018. Substantial changes in air pollution across China during 2015-2017. Environ. Res. Lett. 13. https://doi.org/10.1088/1748-9326/aae718.

Silver, B., He, X., Arnold, S.R., Spracklen, D.V., 2020. The impact of COVID-19 control measures on air quality in China. Environ. Res. Lett. 15, 084021. https://doi.org/10.1088/1748-9326/aba3a2.

Stoerk, T., 2016. Statistical corruption in Beijing's air quality data has likely ended in 2012. Atmos. Environ. 127, 365–371. https://doi.org/10.1016/j.atmosenv.2015.12.055.

Tai, A.P.K., Sadiq, M., Pang, J.Y.S., Yung, D.H.Y., Feng, Z., 2021. Impacts of Surface Ozone Pollution on Global Crop Yields: Comparing Different Ozone Exposure Metrics and Incorporating Co-effects of CO2. Front. Sustain. Food Syst. 5. https://doi.org/10.3389/fsufs.2021.534616.

Tan, Z., Hofzumahaus, A., Lu, K., Brown, S.S., Holland, F., Huey, L.G., Kiendler-Scharr, A., Li, X., Liu, X., Ma, N., Min, K.E., Rohrer, F., Shao, M., Wahner, A.,

Wang, Y., Wiedensohler, A., Wu, Y., Wu, Z., Zeng, L., Zhang, Y., Fuchs, H., 2020. No Evidence for a Significant Impact of Heterogeneous Chemistry on Radical Concentrations in the North China Plain in Summer 2014. Environ. Sci. Technol. 54, 5973–5979. https://doi.org/10.1021/acs.est.0c00525.

Turiel, J.S., Kaufmann, R.K., 2021. Evidence of air quality data misreporting in China: An impulse indicator saturation model comparison of local government-reported and U. S. embassy-reported PM2.5 concentrations (2015–2017). PLOS ONE 16, e0249063. https://doi.org/10.1371/journal.pone.0249063.

van Donkelaar, A., Martin, R.V., Li, C., Burnett, R.T., 2019. Regional Estimates of Chemical Composition of Fine Particulate Matter Using a Combined Geoscience-Statistical Method with Information from Satellites, Models, and Monitors. Environ. Sci. Technol. 53, 2595–2611. https://doi.org/10.1021/acs.est.8b06392.

van Donkelaar, A., Hammer, M.S., Bindle, L., Brauer, M., Brook, J.R., Garay, M.J., Hsu, N.C., Kalashnikova, O.V., Kahn, R.A., Lee, C., Levy, R.C., Lyapustin, A., Sayer, A.M., Martin, R.V., 2021. Monthly Global Estimates of Fine Particulate Matter and Their Uncertainty. Environ. Sci. Technol. 55, 15287–15300. https://doi.org/10.1021/acs.est.1c05309.

Verstraeten, W.W., Neu, J.L., Williams, J.E., Bowman, K.W., Worden, J.R., Boersma, K.F., 2015. Rapid increases in tropospheric ozone production and export from China. Nat. Geosci. 8, 690–695. https://doi.org/10.1038/ngeo2493.

Wang, Z., Uno, I., Yumimoto, K., Itahashi, S., Chen, X., Yang, W., Wang, Z., 2021. Impacts of COVID-19 lockdown, Spring Festival and meteorology on the NO2 variations in early 2020 over China based on in-situ observations, satellite retrievals and model simulations. Atmos. Environ. 244, 117972. https://doi.org/10.1016/j.atmosenv.2020.117972.

Wang, T., Wei, X.L., Ding, A.J., Poon, C.N., Lam, K.S., Li, Y.S., Chan, L.Y., Anson, M., 2009. Increasing surface ozone concentrations in the background atmosphere of Southern China, 1994-2007. Atmospheric Chem. Phys. 9, 6217–6227. https://doi.org/10.5194/acp-9-6217-2009.

Wang, Y., Wild, O., Chen, X., Wu, Q., Gao, M., Chen, H., Qi, Y., Wang, Z., 2020. Health impacts of long-term ozone exposure in China over 2013–2017. Environ. Int. 144, 106030. https://doi.org/10.1016/j.envint.2020.106030.

Wang, S., Xing, J., Zhao, B., Jang, C., Hao, J., 2014. Effectiveness of national air pollution control policies on the air quality in metropolitan areas of China. J. Environ. Sci. China 26, 13–22. https://doi.org/10.1016/S1001-0742(13)60381-2.

Wang, Y., Zhao, Y., Liu, Y., Jiang, Y., Zheng, B., Xing, J., Liu, Y., Wang, S., Nielsen, C.P., 2023. Sustained emission reductions have restrained the ozone pollution over China. Nat. Geosci. 1–8. https://doi.org/10.1038/s41561-023-01284-2.

Wu, H., Tang, X., Wang, Z., Wu, L., Lu, M., Wei, L., Zhu, J., 2018. Probabilistic Automatic Outlier Detection for Surface Air Quality Measurements from the China National Environmental Monitoring Network. Adv. Atmospheric Sci. 35, 1522–1532. https://doi.org/10.1007/s00376-018-8067-9.

Xing, J., Wang, J., Mathur, R., Wang, S., Sarwar, G., Pleim, J., Hogrefe, C., Zhang, Y., Jiang, J., Wong, D.C., Hao, J., 2017. Impacts of aerosol direct effects on tropospheric ozone through changes in atmospheric dynamics and photolysis rates. Atmospheric Chem. Phys. 17, 9869–9883. https://doi.org/10.5194/acp-17-9869-2017.

Xu, F., Huang, Q., Yue, H., Feng, X., Xu, H., He, C., Yin, P., Bryan, B.A., 2023. The challenge of population aging for mitigating deaths from PM2.5 air pollution in China. Nat. Commun. 14, 5222. https://doi.org/10.1038/s41467-023-40908-4.

Xu, W., Lin, W., Xu, X., Tang, J., Huang, J., Wu, H., Zhang, X., 2016. Long-term trends of surface ozone and its influencing factors at the Mt Waliguan GAW station, China-Part 1: Overall trends and characteristics. Atmospheric Chem. Phys. 16, 6191–6205. https://doi.org/10.5194/acp-16-6191-2016.

Yin, S., 2022. Decadal changes in PM2.5-related health impacts in China from 1990 to 2019 and implications for current and future emission controls. Sci. Total Environ. 834, 155334. https://doi.org/10.1016/j.scitotenv.2022.155334.

Yin, P., Brauer, M., Cohen, A., Burnett, R.T., Liu, J., Liu, Y., Liang, R., Wang, W., Qi, J., Wang, L., Zhou, M., 2017. Long-term fine particulate matter exposure and nonaccidental and cause-specific mortality in a large national cohort of Chinese men, 117002–1-117002–11 Environ. Health Perspect. 125. https://doi.org/10.1289/EHP1673.

World Economic Outlook - Real GDP growth, IMF, 2023. URL https://www.imf.org/external/datamapper/NGDP_RPCH@WEO (accessed 4.4.24).

Yin, H., Brauer, M., Zhang, J. (Jim), Cai, W., Navrud, S., Burnett, R., Howard, C., Deng, Z., Kammen, D.M., Schellnhuber, H.J., Chen, K., Kan, H., Chen, Z.-M., Chen, B., Zhang, N., Mi, Z., Coffman, D., Cohen, A.J., Guan, D., Zhang, Q., Gong, P., Liu, Z., 2021. Population ageing and deaths attributable to ambient PM2·5 pollution: a global analysis of economic cost. Lancet Planet. Health 5, e356–e367. https://doi.org/10.1016/S2542-5196(21)00131-5.

Zhang, J. (Jim), Wei, Y., Fang, Z., 2019. Ozone Pollution: A Major Health Hazard Worldwide. Front. Immunol. 10. https://doi.org/10.3389/fimmu.2019.02518.

Zhang, S., Li, Y., Hao, Y., Zhang, Y., 2018. Does public opinion affect air quality? Evidence based on the monthly data of 109 prefecture-level cities in China. Energy Policy 116, 299–311. https://doi.org/10.1016/j.enpol.2018.02.025.

Zhang, Y., Shindell, D., Seltzer, K., Shen, L., Lamarque, J.-F., Zhang, Q., Zheng, B., Xing, J., Jiang, Z., Zhang, L., 2021. Impacts of emission changes in China from 2010 to 2017 on domestic and intercontinental air quality and health effect. Atmospheric Chem. Phys. 21, 16051–16065. https://doi.org/10.5194/acp-21-16051-2021.

Zheng, B., Tong, D., Li, M., Liu, F., Hong, C., Geng, G., Li, H., Li, X., Peng, L., Qi, J., Yan, L., Zhang, Y., Zhao, H., Zheng, Y., He, K., Zhang, Q., 2018. Trends in China's anthropogenic emissions since 2010 as the consequence of clean air actions.

Atmospheric Chem. Phys. 18, 14095–14111. https://doi.org/10.5194/acp-18-14095-2018.

Zheng, B., Zhang, Q., Geng, G., Chen, C., Shi, Q., Cui, M., Lei, Y., He, K., 2021. Changes in China's anthropogenic emissions and air quality during the COVID-19 pandemic in 2020. Earth Syst. Sci. Data 13, 2895–2907. https://doi.org/10.5194/essd-13-2895-2021.

Zhou, M., Wang, H., Zeng, X., Yin, P., Zhu, J., Chen, W., Li, X., Wang, L., Wang, L., Liu, Y., Liu, J., Zhang, M., Qi, J., Yu, S., Afshin, A., Gakidou, E., Glenn, S., Krish, V.S., Miller-Petrie, M.K., Mountjoy-Venning, W.C., Mullany, E.C., Redford, S.B., Liu, H., Naghavi, M., Hay, S.I., Wang, L., Murray, C.J.L., Liang, X., 2019. Mortality, morbidity, and risk factors in China and its provinces, 1990–2017: a systematic analysis for the Global Burden of Disease Study 2017. The Lancet 394, 1145–1158. https://doi.org/10.1016/S0140-6736(19)30427-1.